Amyloid, December 2006; 13(4): 226–235

informa
healthcare

FALS mutations in Cu, Zn superoxide dismutase destabilize the dimer and increase dimer dissociation propensity: A large-scale thermodynamic analysis

SAGAR D. KHARE, MICHAEL CAPLOW, & NIKOLAY V. DOKHOLYAN

Department of Biochemistry & Biophysics, University of North Carolina at Chapel Hill, School of Medicine, Chapel Hill, NC 27599, USA

Keywords: *Amyotrophic lateral sclerosis, Cu, Zn superoxide dismutase, aggregation, stability, dimer dissociation, molecular dynamics simulations*

Abbreviations: *ALS = amyotrophic lateral sclerosis; FALS = familial amyotrophic lateral sclerosis; MD = molecular dynamics; RMSD = root mean square deviation*

Abstract

Mutations in the dimeric enzyme Cu, Zn superoxide dismutase (SOD1) leading to its aggregation are implicated in the toxicity in familial amyotrophic lateral sclerosis (FALS). We and others have previously shown that aggregation occurs by a pathway involving dimer dissociation, metal-loss from monomers and multimeric assembly of apo-SOD1 monomers. We postulate that FALS mutations cause enhanced aggregation by affecting one or more steps in the pathway, and computationally test this postulate for 75 known mis-sense FALS mutants of SOD1. Based on an extensive thermodynamic analysis of the stability of apo-dimer and apo-monomer forms of these mutants, we classify the mutations into the following groups: 70 out of 75 mutations in SOD1 lead to (i) decreased dimer stability, and/or (ii) increased dimer dissociation, compared to wild type, and four mutations lead to (iii) decreased monomer stability compared to wild type. Our results suggest that enhanced aggregation of SOD1 in FALS occurs due to an increased population of mutant SOD1 apo-monomers compared to wild type. The dissociation of multimeric proteins induced by diverse mutations may be a common theme in several human diseases.

Introduction

Point mutations in the cytoplasmic homodimeric enzyme Cu, Zn superoxide dismutase have been identified as the primary cause of approximately 20% cases of the disease Familial ALS [1–4]. More than 90 distinct and structurally diverse FALS mutations are known [5]. The sporadic form of ALS (SALS), which is not associated with any heritable defect, constitutes ≈90% of all ALS cases and is symptomatically identical to SOD1-linked FALS. It is likely that understanding the molecular basis of SOD1-linked FALS will also provide insights for understanding SALS [6].

There is increasing evidence that the FALS does not arise due to a reduction in mutant SOD1 activity [7,8], and the motor neuron-specific toxic gain-of-function of the mutants is associated with intracellular aggregation, trafficking and/or degradation of misfolded SOD1 [9,10]. The mutation-induced destabilization of the native state of SOD1 may lead to a relatively higher population of misfolded or partially folded protein molecules that may (i) assemble into structured fibrils [11], (ii) interfere with mitochondrial transport [12], and/or (iii) saturate the protein degradation machinery [13], thereby leading to toxicity. Thus, the misfolding-induced aggregation of mutant SOD1 leading to the appearance of inclusion bodies is correlated with toxicity, and the inhibition of aggregation by over-expression of chaperones leads to increased cell viability [14].

The molecular mechanism of misfolding and aggregation of SOD1 is not well-understood. We and others have previously provided evidence that the aggregation of SOD1 occurs via a pathway involving dissociation [15,16] of the dimer and metal-loss, followed by multimeric assembly of the apo-monomeric SOD1[15]. Mutations are likely to lead to enhanced aggregation by affecting one or more steps in the pathway. *In vivo*, FALS mutant SOD1s have decreased solubility and half-life compared to

Correspondence: Nikolay V. Dokholyan. Tel: +1 919 843 2513. Fax: +1 919 966 2852. E-mail dokh@med.unc.edu

ISSN 1350-6129 print/ISSN 1744-2818 online © 2006 Informa UK Ltd.
DOI: 10.1080/13506120600960486

wild type, indicating that they form less stable dimers. Also, SOD1 solvent denaturation occurs via a monomeric intermediate [17,18], this monomeric intermediate was also detected in the oxidation-induced aggregation of wild type SOD1. Preventing dimer dissociation by engineering an inter-subunit disulfide bond abolished the aggregation of the A4V FALS SOD1 mutant. Evidence that the apo-form of mutant SOD1 is involved in FALS-linked pathology is (i) the *in vitro* stability of the mutant apo-dimers was correlated with the mean survival time of FALS patients carrying the mutation [19], (ii) treatment of ALS patients with chelators such as penicillamine, EDTA, and thioctic acid was found to sometimes accelerate the disease, (iii) the *in vitro* aggregation rate of A4V and H43R SOD1 was enhanced in the presence of EDTA [20], and (iv) some recombinant mutant SOD1s were found to have smaller metal content and stability than wild type [21]. Taken together, these studies suggest a general framework for the effect of mutation on FALS-linked aggregation of SOD1, in which mutations cause enhanced aggregation by decreasing apo-SOD1 dimer and monomer stability and/or increasing dimer dissociation, compared to the wild type. An exhaustive analysis of FALS mutants is required to test this general framework. In spite of the recent significant advances [19,22–25], the challenging task of uncovering the effect of mutation on dimer-monomer equilibrium of apo-SOD1 is likely to remain experimentally unfeasible on the large scale required to ascertain the generality of the suggested framework.

Here, we perform exhaustive *in silico* mutagenesis of SOD1 and evaluate the dimer stabilities and dissociation propensities for 75 FALS-associated point mutants in SOD1 using molecular dynamic (MD) simulations and an implicit-solvation based scoring function. The effect of mutation on SOD1 dimer stability is evaluated as the difference in the calculated conformational free energy between mutant and wild type SOD1, and the dissociation propensity is evaluated as the difference between the conformational free energies of the SOD1 dimer and two monomers. Based on these calculations, we classify mutants into four groups depending upon how mutation affects dimer stability and dimer dissociation. We find that 70 out of 75 FALS mutants decrease dimer stability and/or increase dimer dissociation, while four of the remaining five lead to decreased monomer stability.

Methods

Generating mutant SOD1 structures

The available structures of mutant SOD1 molecules show remarkable similarity and are almost identical to the wild-type (RMSD ≤ 1.25 Å); the difference between wild-type and mutant SOD1 molecules is largely due to side-chain packing [26–29]. Thus, we generate mutant structures by *in silico* mutation using the package Sybyl (Tripos Inc.) and the wild-type SOD1 structure (PDB accession code: 1SPD) keeping the backbone coordinates fixed and replacing the appropriate side-chains. This procedure is followed by 200 steps of steepest descent energy minimization in the vicinity of mutation to remove steric clashes, while the rest of the protein is rigid.

Estimating conformational free energy

We determine the conformational free energy of a structure by the Explicit Solvent Implicit Solvent (ES/IS) method as described by Vorobjev et al. [30–33]. Applied to SOD1, the method consists of a short molecular dynamics simulation (196 ps) of SOD1 (wild-type or mutant) with explicit solvent (ES) to obtain microstates of the system. The conformational free energy of the SOD1 structure is written as a sum of six contributions:

$$G = \langle U_{m,sh} \rangle + \langle U_{m,coul} \rangle - TS_{conf} + \langle G_{cav} \rangle + \langle G_{s,vdw} \rangle + \langle G_{pol} \rangle, \quad (1)$$

where $\langle \ldots \rangle$ denotes average over the MD trajectory, U_m is the intra-protein conformational energy which can be written as the sum of short-range, $U_{m,sh}$, and coulombic, $U_{m,coul}$, terms, S_{conf} is the determined conformational entropy, and T is the absolute temperature. The solvation free energy, G_{sol}, is a sum of the last three terms: the free energy of creating the empty protein-sized cavity in the solvent G_{cav}, the free energy of inserting the protein molecule into the protein-sized cavity $G_{s,vdw}$, and the free energy of solvent polarization G_{pol}. $\langle U_m \rangle$ and $\langle G_{s,vdw} \rangle$ is accumulated as averages during the molecular dynamics simulation. S_{conf} is calculated from the position covariance matrix of the protein during the dynamics trajectory in the quasi-harmonic approximation. G_{cav} and G_{pol} is calculated with models in which the solvent is treated implicitly, as described by Vorobjev and Hermans [33]. Thus, this gives a physically realistic energy function that effectively discriminates between wild-type and mutant SOD1 structures.

Estimation of the effect of a mutation on SOD1 stability requires knowledge of the free energy of the reference (unfolded) states of the wild type G_U^{WT} and mutant G_U^X molecules. The stability of the wild type or a mutant SOD1 is then determined by the following:

$$\Delta G^{WT} = G_N^{WT} - G_U^{WT}, \quad (2)$$

and

$$\Delta G^X = G_N^X - G_U^X. \quad (3)$$

We thus determine the change in SOD1 stability due to a mutation:

$$\Delta\Delta G^X = \Delta G^X - \Delta G^{WT} = \left(-G_N^{WT} + G_N^X\right) + \left(G_U^{WT} - G_U^X\right). \quad (4)$$

We assume that the reference (unfolded) state can be modeled as a fully solvated chain. We determine these by computing the conformational free energy G_U of the small peptides Ace–$(Ala)_2$–Gly–Ala–x–Ala–Gly–$(Ala)_2$–NMet using the ES/IS method, where x denotes any of 20 amino acids (Table I). Thus, we calculate the conformational free energy difference between wild-type and mutant SOD1 for monomeric $\Delta\Delta G_m^X$, dimeric $\Delta\Delta G_d^X$.

The dimer dissociation is characterized by comparing the free energies of monomers and the dimer:

$$\Delta G_{dissoc} \approx -(G_{dim} - 2G_{mono}) \quad (5)$$

where ΔG_{dissoc} is the free energy of dimer dissociation, G_{dim} and G_{mono} are the ES/IS free energies of the dimer and monomer, respectively.

All molecular dynamic (MD) calculations are performed using the Sigma molecular dynamics program [34] and the CEDAR force field using a protocol involving relaxation and production, as described elsewhere [35].

The uncertainty (error-bar) in the estimated free energy is ideally obtained by performing multiple simulations and calculating the dispersion of the average values thus obtained. For the D90A mutant, the average free energies obtained in two independent simulations are −7353.5 and −7332.0 kcal/mol (difference = 21.5 kcal/mol). The difference between the D90A mutant and wild type is 175.8 kcal/mol, and therefore we estimate the values reported have an intrinsic uncertainty of approximately 15%.

Results and discussion

MD trajectories

Molecular dynamic simulations of mutant SOD1 structures generated from the wild type are performed for 196 ps and snap shots are recorded every 2 ps yielding a total of 98 snapshots. The conformational free energy of the mutant is calculated as the average of the conformational free energies of the 98 snapshots. All the SOD1 MD trajectories are stable in our simulations and sample conformations that are near-native (RMSD < 2.5 Å). For four representative mutant dimers and monomers, RMSD *versus* time is shown in Figure 1(a). We find that the monomers have a larger RMSD, which is expected since monomerization exposes a large hydrophobic patch on the surface of SOD1 to the solvent. However, both the dimers and monomers are stable on the time-scale of the simulation (200 ps). This is in accord with the observation that the SOD1 unfolding occurs *via* a monomeric intermediate, and the stability of the monomer is ∼4 kcal/mol,

Table I. Free energies of the unfolded state.

x	$U_{m,sh}$	$U_{m,coul}$	G_{cav}	$G_{s,vdw}$	G_{pol}	G_{solv}	TS_{conf}	G
Ala	31	0.8	43.2	−35.2	−39.3	−31.3	−18.70	3.76
Arg	39	−14	49.4	−37.7	−96.3	−84.7	−19.77	−57.50
Asn	33.1	−40.9	45.5	−35.2	−46.2	−35.9	−18.10	−39.92
Asp	58	−9.7	46.1	−29.1	−122.8	−105.8	−21.42	−56.94
Cys	55.5	−2.5	45.5	−37	−39	−30.5	−18.63	25.836
Gln	35.1	−36.4	47.4	−35.9	−50.9	−39.4	−18.92	−37.65
Glu	34.6	−5.4	45.8	−29.7	−127.5	−111.4	−23.77	−84.00
Gly	31.6	−2.8	43.3	−36	−38.2	−30.9	−19.77	0
His	32.9	−17.3	46.8	−38.2	−46.2	−37.5	−19.03	−18.95
Ile	38.5	−5.2	45.8	−38.3	−34.9	−27.4	−18.17	9.69
Leu	36.6	−5.6	46.6	−38.9	−34.3	−26.6	−20.39	5.97
Lys	67	1	48.9	−31.1	−133.2	−115.3	−20.50	−45.83
Met	34	−6.1	47.8	−40.2	−34.5	−26.9	−19.32	3.64
Phe	35	−0.3	47.1	−41.5	−38.9	−33.2	−19.61	3.86
Pro	44.4	−0.6	45.7	−38.6	−38.5	−31.4	−22.36	12.0
Ser	32.7	−3.7	44.1	−32.8	−46.5	−35.2	−21.37	−5.60
Thr	35	−7.5	45.9	−36	−43.3	−33.4	−22.60	−6.53
Trp	36.2	−2.9	50.1	−44.9	−41.4	−36.2	−19.38	−0.31
Tyr	35.2	−9.9	48.7	−40.1	−41	−32.3	−19.31	−4.34
Val	62.1	−4	46.3	−36.9	−37.4	−28	−20.09	31.97

Free energies of peptides (Ace–$(Ala)_2$–Gly–Ala–x–Ala–Gly–$(Ala)_2$–NMet) relative to x = Gly.

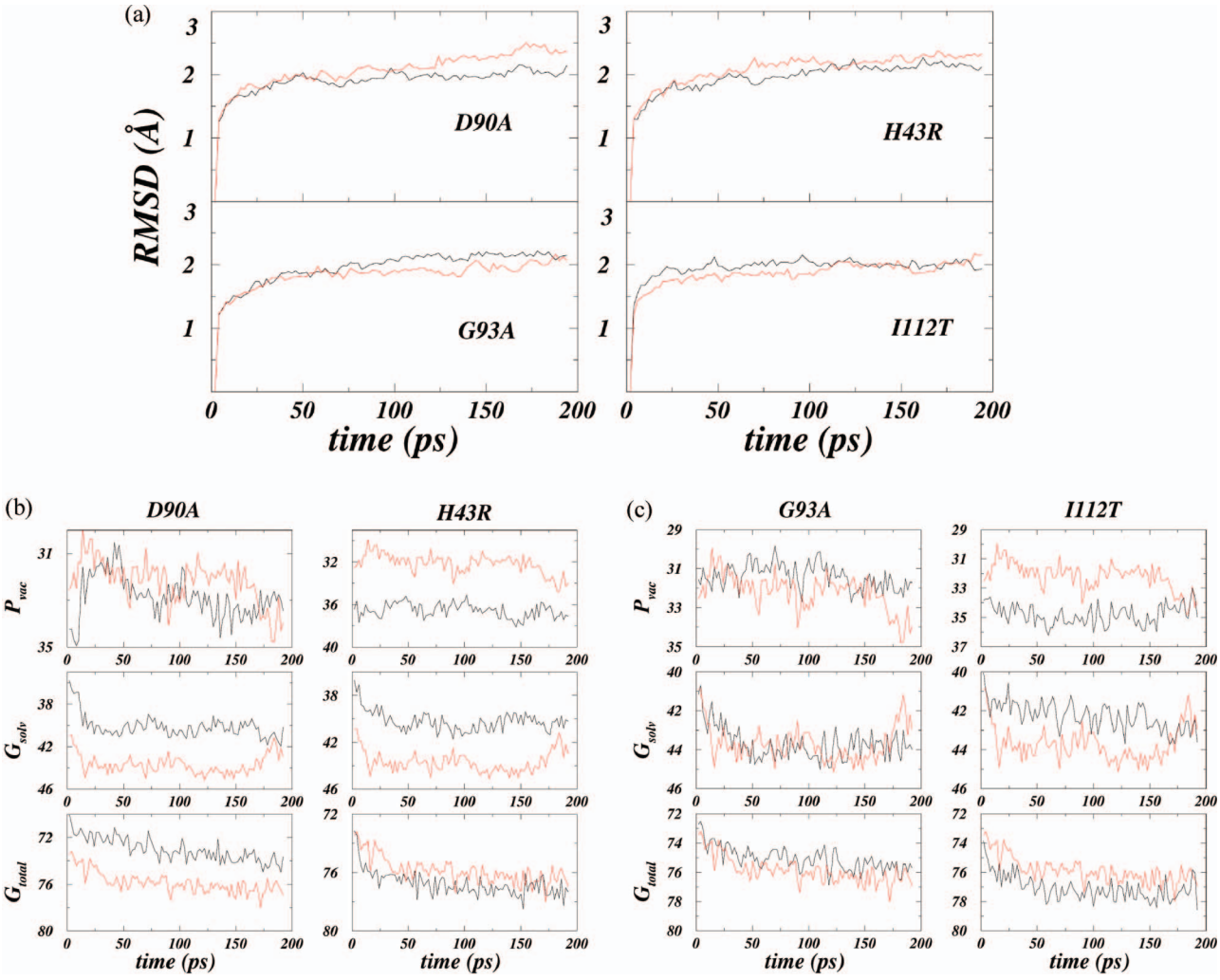

Figure 1. Conformational free energies of 75 FALS point mutants (a) The C_α-RMSD versus time for four representative mutant trajectories. The dimer is in black and monomer in red. (b and c) The internal energy, solvation free energy and total conformational free energy for the four mutants in (a). For comparison, the wild type energies are shown in red.

thus the monomers are expected to be stable on a picosecond timescale.

Conformational free energy calculations and classification of mutants

Based on a free-energy cycle thermodynamic analysis (Methods) we estimate the change in free energy change ($\Delta\Delta G_{dim} = \Delta G^{mut}_{dim} - \Delta G^{WT}_{dim}$) for unfolding between the mutant and Wild-type dimer structures. $\Delta\Delta G_{dim}$ is a measure of the tendency of the mutant dimer to unfold relative to the wild type. The effect of mutation on the stability can be construed as arising from both effects on intra-protein interactions, and protein–water interactions (solvation). We find that in mutations such as D90A and G93A (Figure 1b), the destabilizing effect of mutation is due to the decreased solvation energy relative to wild type (shown as red curves in Figure 1b); the intra-protein interactions (in vacuum) are not significantly affected. For other mutants such as I112T, which stabilizes the dimer, the intra-protein interaction energy is higher than the wild type, whereas the solvation free energy is lower or of similar magnitude (Figure 1b). This is in accord with the experimental finding that SOD1 FALS mutants have lower solubility *in vivo* than the wild type protein. We find that the differences between mutant and wild type dimers are statistically significant and we obtain distinct distributions in the Kolomogorov–Smirnov test (data not shown).

Since SOD1 is a dimer, the stability change upon mutation in the dimer is $\Delta\Delta G_{dim} = -\Delta\Delta G_{dissoc} + 2\Delta\Delta G_{monomer}$, where $\Delta\Delta G_{dissoc}$ and $\Delta\Delta G_{monomer}$ are the change in dissociation free energy and the change in monomer stability, respectively. The values of $\Delta\Delta G_{dissoc}$ and $\Delta\Delta G_{dim}$ are expected to be anti-correlated. We evaluate the tendency of the mutant

SOD1 to dissociate into its monomeric subunits, which we estimate by change in dissociation free energy change between mutant and wild type. The more negative this value, the higher the dissociation tendency and the higher is the chance that the mutant forms the monomeric state. This apo-monomer, in turn, is likely to form misfolded/unfolded structures that aggregate. Thus, we characterize each mutant by its $\Delta\Delta G_{dim}$ and $\Delta\Delta G_{dissoc}$ values (Figure 2) and classify the mutants into four different classes based on their effect on dimer stability and dissociation relative to wild type (Figure 2 and Table II): Class I (lower dimer stability, increased dimer dissociation, e.g. D90A), Class II (higher dimer stability, increased dimer dissociation, e.g.) – this class of mutations may stabilize the dimer relative to the unfolded state but stabilize the monomer to a greater degree, Class III (lower dimer stability, decreased dimer dissociation, e.g., H80R) – this class of mutations may destabilize the dimer relative to the unfolded state but destabilize the monomer to a greater extent, and Class IV (higher dimer stability, decreased dimer dissociation, e.g., I112T), mutants, respectively. In total, all but 15 out of the 75 mutants destabilize the dimer, while all but 10 are more prone to dissociate than the wild type. Five of the 75 mutants marginally stabilize the dimer as well as increase dimer dissociation propensity, but the monomers of these mutants have lower stability than the wild type monomer. Therefore, we conclude that FALS mutations in SOD1 may induce aggregation by one or more of the following: (i) decreasing dimer stability, (ii) decreasing monomer stability, and (iii) increasing dimer dissociation propensity. A mutation belonging to each class, affects the dimer-monomer equilibrium such that the overall equilibrium is shifted towards the apo-monomer, and thus increases the population of the aggregation-prone species.

Comparison with experiments

Although the free energy estimates obtained from short MD simulations do not yield accurate magnitude of the free energy changes upon mutation, they suggest that most FALS SOD1 mutations destabilize the dimer and/or the monomer. The destabilization of SOD1 has been observed in a subset of FALS mutants previously. We compare the changes in stability obtained from MD simulations with the experiments of Rodriguez et al. [21] (Figure 3) and Lindberg et al. [19] to estimate the agreement of the calculated and measured free energies. Rodriguez et al. [21] report four peaks in the DSC scans of the SOD1 mutants, and the peak with the lowest melting temperature (T_m) corresponds to the metal-free SOD1 species. We compare our $\Delta\Delta G_{dim}$ values with the ΔT_m values of the corresponding 15 FALS mutants and find reasonable agreement. We correctly identify the mutations that do not have any

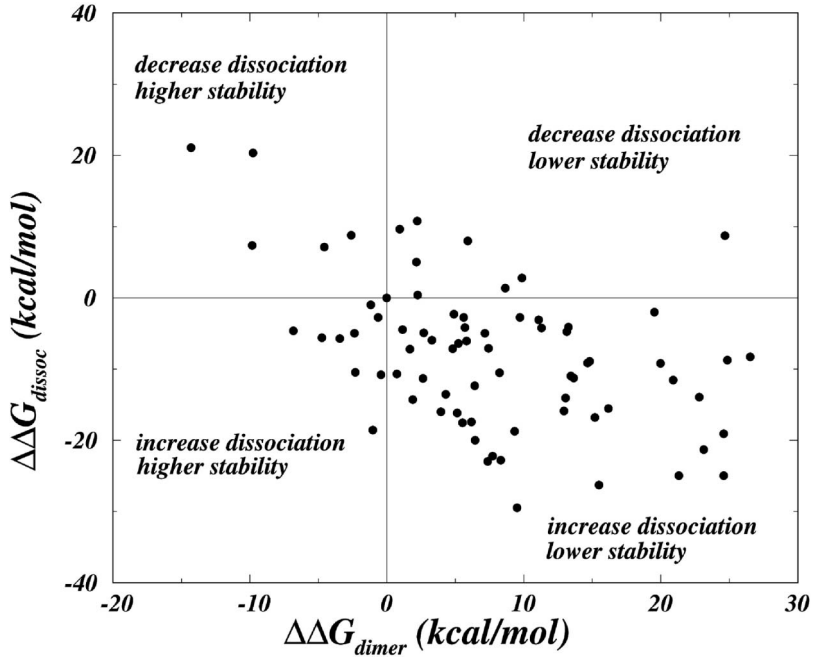

Figure 2. The effect of mutation on SOD1 dimer stability and dissociation for all 75 FALS mutants considered in this study. 70 out of 75 mutations lower dimer stability and/or increase dimer dissociation, whereas five out of 75 lead to marginally higher stability and decreased dimer dissociation.

Table II. Conformational Free Energies of SOD1 mutants.

Res(wild type)	Pos	Res(Mut)	$\Delta\Delta G$(dim-s)	$\Delta\Delta G$(dissoc-s)
Class I				
Wild type			0	0
A	4	S	9.737	−2.73
A	4	T	11.128	−3.068
A	4	V	13.468	−10.985
V	7	E	9.529	−29.471
L	8	V	2.73	−4.94
G	12	R	6.201	−17.446
V	14	G	14.69	−9.126
V	14	M	2.197	5.005
G	16	A	9.373	−18.72
G	16	S	2.236	10.816
E	21	G	11.323	−4.199
G	37	R	6.461	−19.994
L	38	R	1.924	−14.287
L	38	V	7.189	−4.953
G	41	S	6.435	−12.311
H	46	R	3.965	−16.003
H	48	Q	0.754	−10.66
E	49	K	7.397	−22.932
N	65	S	13.286	−4.134
D	76	V	20.007	−9.204
D	76	Y	24.908	−8.723
L	84	F	4.329	−13.546
L	84	V	15.535	−26.299
G	85	R	13.182	−4.719
N	86	S	14.833	−8.931
A	89	V	13.078	−14.027
D	90	A	22.854	−13.936
D	90	V	23.179	−21.294
G	93	C	4.914	−2.288
G	93	R	5.629	−2.756
G	93	V	13.676	−11.258
A	95	T	5.837	−6.071
D	96	N	19.565	−1.976
D	101	G	26.559	−8.268
D	101	N	24.635	−24.986
S	105	L	4.823	−7.137
L	106	V	7.449	−7.085
G	108	V	5.252	−6.422
D	109	N	21.346	−24.973
I	112	M	8.359	−22.802
I	113	F	3.315	−5.915
I	113	T	2.652	−11.336
G	114	A	12.948	−15.873
R	115	G	20.943	−11.544
D	124	V	16.198	−15.509
D	125	H	15.21	−16.77
L	126	S	5.564	−17.524
S	134	N	2.262	0.39
L	144	F	1.183	−4.472
A	145	G	8.268	−10.517
A	145	T	24.622	−19.084
C	146	R	7.748	−22.191
V	148	G	5.733	−4.147
V	148	I	5.161	−16.146
I	149	T	1.703	−7.189
Class II				
L	8	Q	−0.611	−2.73
G	41	D	−1.001	−18.564
H	43	R	−6.812	−4.602
L	67	R	−3.419	−5.694
H	80	R	−4.732	−5.59
V	97	M	−0.416	−10.79
I	104	F	−1.131	−0.949
N	139	K	−2.327	−4.966
L	144	S	−2.288	−10.426
Class III				
G	10	V	5.941	7.995
G	72	S	8.684	1.378
G	93	A	9.906	2.795
E	100	G	24.726	8.736
I	151	T	0.975	9.633
Class IV				
E	21	K	−4.55	7.163
G	93	D	−9.815	7.358
G	93	S	−2.561	8.775
E	100	K	−9.737	20.358
I	112	T	−14.274	21.086

effect on stability (H48Q), as well as those which have a large effect on stability, thus covering a range of stability values. However, there is disagreement in the trends between the experimentally measured and computed degrees of destabilization. We find that the trend in the magnitude of destabilization caused by mutations on the surface of SOD1 (G93A, G93S) is significantly different between experiment and our results, whereas the trend in the magnitudes of more buried mutations (H48Q, A4V) is similar in experiments and our results. Since, surface residues in proteins are more labile than buried ones, it is likely that a 200-ps time-window is not sufficient for convergence. The lack of convergence may lead to inaccuracies in estimating the magnitudes of destabilization caused by mutation, particularly when a small side chain is replaced by a larger one (G93A, G93S). Therefore, we conclude that free energy estimates obtained from our method can indicate whether a mutation is destabilizing or stabilizing in partial agreement with experiments, but accurately estimating the magnitude of destabilization requires a greater amount of sampling.

Similarly, for the data of Lindberg et al. [19], we find qualitative agreement between the estimated free energy values, and the change in mid-point concentration of urea, for the melting curve obtained in their experiments. Similar qualitative, albeit slightly worse, agreement is found with other recent stability measurements [36,37]. Our simulations rely on the assumption that there is no major structure change upon mutation, and in accord with this assumption, we find that the simulated structures are within 1.8 Å RMSD, of the experimentally determined FALS mutants (Figure 4). Thus, while the free energies obtained in simulations do not quantitatively agree with the experimental data completely, they provide support for the hypothesis that most FALS SOD1 mutations destabilize SOD1.

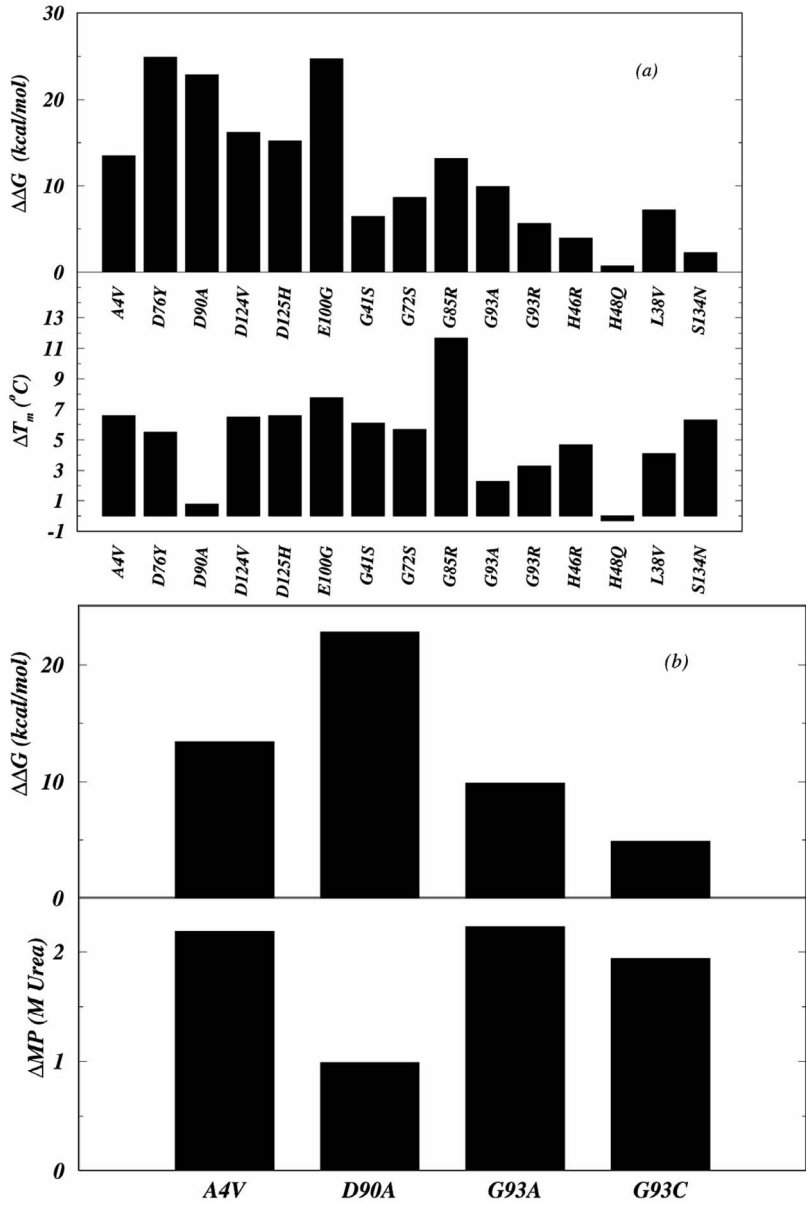

Figure 3. Comparison of calculated free energies with experiments. (a) Comparison of calculated $\Delta\Delta G$ with change in melting temperature (ΔT_m) for 15 FALS mutants. ΔT_m is obtained from Rodriguez et al. [21]. (b) Comparison of calculated $\Delta\Delta G$ with change in mid-point Urea concentration during solvent denaturation (ΔMP^{ap}) for four FALS mutants. ΔMP^{ap} is obtained from Lindberg et al. [19].

Qualitative analysis of aggregation propensity

Serrano and co-workers have developed the algorithm TANGO [38] which predicts the propensity of local sequence stretches in a protein or peptide to aggregate. For wild type SOD1, TANGO predicts that the residues at the N- and C-terminus, 1–9 and 141–152, respectively, are regions of high aggregation propensity. In the SOD1 dimer structure, the terminal residues are protected and form a part of the dimer interface. Mutations close to or on the dimer interface (e.g., A4V) are predicted to increase the aggregation propensity of the terminal residues themselves. Our analysis here and previously published results [39,40] suggest that mutations away from the dimer interface, e.g., in the metal-binding region, may increase the dimer dissociation propensity, and therefore cause the exposure of the aggregation-prone terminal residues. These exposed terminal residues may aberrantly interact with other monomers to induce aggregation. Thus, a qualitative analysis of aggregation hot-spots in SOD1 suggests that FALS mutations may induce the aggregation of SOD1 by two mechanisms: dimer-interface mutations may directly enhance the aggregation propensity of hot-spot regions, whereas other mutations may destabilize the dimer, thereby exposing the aggregation hot-spots.

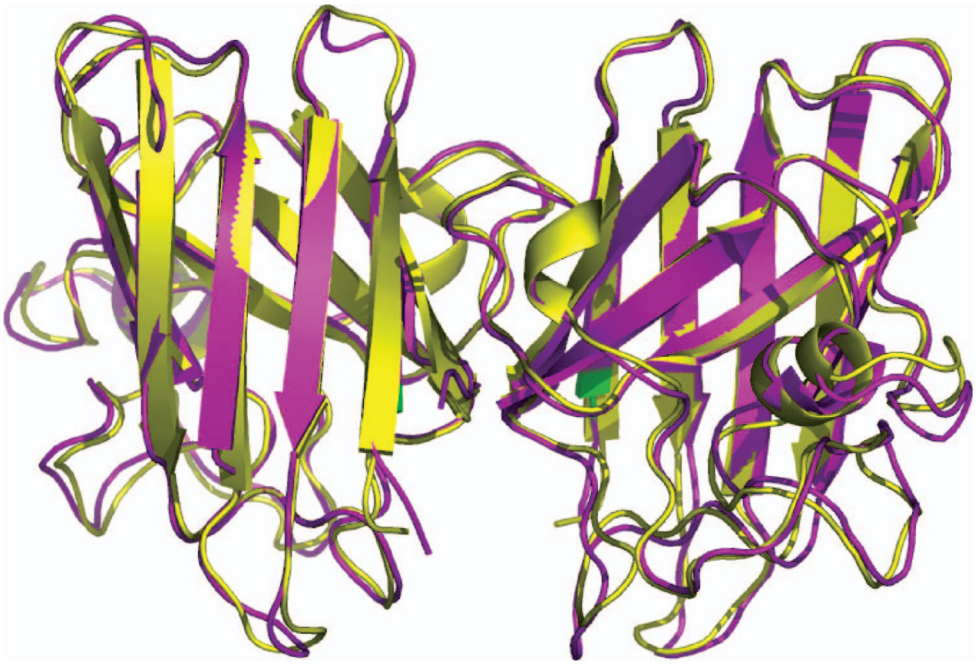

Figure 4. Superimposition of SOD1 structures. Structural identity is seen between solved crystal structures of A4V (1UXM, pink) and the modeled structure (yellow). The site of mutation, Ala4, is shown in green.

Dissociation of multimeric proteins in other human diseases

The dissociation of multimeric proteins has been implicated in several human diseases [41]. More than 80 mutations in the tetrameric protein transthyretin (TTR) are linked to its familial amyloidosis. All disease-associated mutations in the tetrameric protein TTR were found to enhance its amyloidosis by inducing dissociation of the native tetramer – a so-called 'kinetic destabilization' since the rate of aggregation is determined by the rate of tetramer dissociation [42]. These mutations are scattered throughout the structure of the 127-residue TTR monomer, and are likely to induce tetramer dissociation by long-range effects on the tetramer interface, similar to the effect of FALS mutants on the SOD1 dimer interface. The relative stabilities of the TTR tetramer and monomers with respect to the unfolded state determine the propensity (and rate, since the association reaction is near diffusion-limited) of wild type or mutant TTR to form the aggregation-prone monomer. Thus, similar to SOD1 dimer and monomer stabilities, the effect of mutations on TTR stability may underlie its aggregation in systemic amyloidosis.

Oligomerization of human cystatin C leads to amyloid deposits in brain arteries. It is known that cystatin C exists as a dimer, formed during intracellular trafficking [43], and is converted to monomer at or before secretion. It has been shown that the monomers can re-dimerize [44] via three-dimensional (3D) domain swapping, and this observation has led to the suggestion that an analogous domain-swapping mechanism, but propagated in an open-ended fashion, could be the basis of fibril formation. Thus, the dimer dissocation of cystatin C may be implicated in its aggregation in disease.

More than 234 missense point mutations in the tetrameric enzyme phenylalanine hydroxylase (PAH) are implicated in hyperphenylalaninemia [45]. Few mutants directly abolish the activity, and a large majority is implicated in altering the stability and degradation of the enzyme. Several mutations in sites distant from both the active site, and the tetramer interface, were shown have a destabilized tetrameric state, and were aggregation-prone *in vitro* [46]. These mutations were found to promote misfolding of the PAH monomer and oppose correct assembly of monomers into the native tetrameric enzyme [47]. This suggests that, similar to SOD1, the long-range destabilization of the tetramer interface through the network of contact interactions may be implicated in a subset of the cases of the disease.

Similarly, rare mutations in the protein DL-1 involved in Parkisnson's disease are known to destabilize the native dimer [48]. In the protein α-crystallin, which is upregulated in several neurodegenerative diseases, post-translational phosphorylation at distinct sites, presumably distal from the dimer interface [49], is known to cause dimer destabilization and aggregation of the protein leading to loss of chaperone activity [50]. The loss of activity has been postulated to disrupt the housekeeping function of this protein, and thus may be significant for neurodegenerative diseases. Therefore, the mutation-induced destabilization of the multimeric

structure, by the long-range transduction of signals, may be a common theme in the mechanism by which deleterious SNPs lead to human disease.

In conclusion, how unrelated mutations in SOD1 cause FALS represents a major challenge for delineating the molecular mechanism of the disease. Based on a large-scale thermodynamic analysis of the stabilities of 75 mutants, we find that 70 out of the 75 mutants modulate aggregation propensity by decreasing overall SOD1 stability and/or increasing dimer dissociation. A graph theoretic analysis of SOD1 also reveals that sites in the protein are highly connected to the dimer interface and the metal-binding sites, suggesting that a mutation-induced perturbation is likely to cause dimer dissociation and metal-loss [39]. Thus, in a unified framework to account for the effect of all FALS mutations on SOD1 dimer, we propose that mutations lead to enhanced aggregation by increasing the population of the apo-monomer by (a) decreasing overall dimer stability, and/or (b) increasing dimer dissociation propensity, and/or (c) decreasing monomer stability. This framework may be the underlying basis for a subset of phenotypic effects in other diseases in which seemingly structurally unrelated mutations in multimeric proteins are involved.

Acknowledgements

We thank G. Butterfoss, H. Hu and J. Hermans for help with Sigma and ES/IS methods. We thank B. Kuhlman for helpful discussions.

References

1. Valentine JS, Doucette PA, Potter SZ. Copper-zinc superoxide dismutase and amyotrophic lateral sclerosis. Ann Rev Biochem 2005;74:563–593.
2. Bruijn LI, Miller TM, Cleveland DW. Unraveling the mechanisms involved in motor neuron degeneration in ALS. Ann Rev Neurosci 2004;27:723–749.
3. Cleveland DW, Rothstein JD. From Charcot to Lou Gehrig: Deciphering selective motor neuron death in ALS. Nat Rev Neurosci 2001;2:806–819.
4. Cleveland DW. From Charcot to SOD1: Mechanisms of selective motor neuron death in ALS. Neuron 1999;24:515–520.
5. Gaudette M, Hirano M, Siddique T. Current status of SOD1 mutations in familial amyotrophic lateral sclerosis. Amyotrophic Lateral Sclerosis Other Motor Neuron Disord 2000;1:83–89.
6. Camu W, Khoris J, Moulard B, Salachas F, Briolotti V, Rouleau GA, Meininger V. Genetics of familial ALS and consequences for diagnosis. J Neurol Sci 1999;165.
7. Cleveland DW, Liu J. Oxidation versus aggregation – how do SOD1 mutants cause ALS? Nat Med 2000;6:1320–1321.
8. Gong YH, Parsadanian AS, Andreeva A, Snider WD, Elliott JL. Restricted expression of G86R Cu/Zn superoxide dismutase in astrocytes results in astrocytosis but does not cause motoneuron degeneration. J Neurosci 2000;20:660–665.
9. Wang J, Slunt H, Gonzales V, Fromholt D, Coonfield M, Copeland NG, Jenkins NA, Borchelt DR. Copper-binding-site-null SOD1 causes ALS in transgenic mice: aggregates of non-native SOD1 delineate a common feature. Hum Mol Genet 2003;12:2753–2764.
10. Wang J, Xu G, Borchelt DR. High molecular weight complexes of mutant superoxide dismutase 1: age-dependent and tissue-specific accumulation. Neurobiol Dis 2002;9:139–148.
11. Johnston JA, Dalton MJ, Gurney ME, Kopito RR. Formation of high molecular weight complexes of mutant Cu,Zn-superoxide dismutase in a mouse model for familial amyotrophic lateral sclerosis. PNAS 2000;97:12571–12576.
12. Liu J, Lillo C, Jonsson PA, Velde CV, Ward CM, Miller TM, Subramaniam JR, Rothstein JD, Marklund S, Andersen PM, Brannstrom T, Gredal O, Wong PC, Williams DS, Cleveland DW. Toxicity of familial ALS-linked SOD1 mutants from selective recruitment to spinal mitochondria. Neuron 2004;43:5–17.
13. Patel YJ, Payne S, de BJ, Latchman DS. Hsp27 and Hsp70 administered in combination have a potent protective effect against FALS-associated SOD1-mutant-induced cell death in mammalian neuronal cells. Brain Res Mol Brain Res 2005;134:256–274.
14. Kieran D, Kalmar B, Dick JR, Riddoch-Contreras J, Burnstock G, Greensmith L. Treatment with arimoclomol, a coinducer of heat shock proteins, delays disease progression in ALS mice. Nat Med 2004;10:402–405.
15. Khare SD, Caplow M, Dokholyan NV. The rate and equilibrium constants for a multistep reaction sequence for the aggregation of superoxide dismutase in amyotrophic lateral sclerosis. PNAS 2004;101:15094–15099.
16. Ray SS, Nowak RJ, Strokovich K, Brown RH, Walz T, Lansbury PT. An intersubunit disulfide bond prevents in vitro aggregation of a superoxide dismutase-1 mutant linked to familial amytrophic lateral sclerosis. Biochemistry 2004;43:4899–4905.
17. Mei G, Rosato N, Silva N, Rusch R, Gratton E, Savini I, FinazziAgro A. Denaturation of human Cu,Zn superoxide-dismutase by guanidine-hydrochloride – a dynamic fluorescence study. Biochemistry 1992;31:7224–7230.
18. Stroppolo ME, Malvezzi-Campeggi F, Mei G, Rosato N, Desideri A. Role of the tertiary and quaternary structures in the stability of dimeric copper,zinc superoxide dismutases. Arch Biochem Biophys 2000;377:215–218.
19. Lindberg MJ, Tibell L, Oliveberg M. Common denominator of Cu/Zn superoxide dismutase mutants associated with amyotrophic lateral sclerosis: Decreased stability of the apo state. Proc Natl Acad Sci USA 2002;99:16607–16612.
20. DiDonato M, Craig L, Huff ME, Thayer MM, Cardoso RMF, Kassmann CJ, Lo TP, Bruns CK, Powers ET, Kelly JW, Getzoff ED, Tainer JA. ALS mutants of human superoxide dismutase form fibrous aggregates via framework destabilization. J Molec Biol 2003;332:601–615.
21. Rodriguez JA, Valentine OS, Eggers DK, Roe JA, Tiwari A, Brown RH, Hayward LJ. Familial amyotrophic lateral sclerosis-associated mutations decrease the thermal stability of distinctly metallated species of human copper/zinc superoxide dismutase. J Biol Chem 2002;277:15932–15937.
22. Rakhit R, Crow JP, Lepock JR, Kondejewski LH, Cashman NR, Chakrabartty A. Monomeric Cu,Zn-superoxide dismutase is a common misfolding intermediate in the oxidation models of sporadic and familial amyotrophic lateral sclerosis. J Biol Chem 2004;279:15499–15504.
23. DiDonato M, Craig L, Huff ME, Thayer MM, Cardoso RMF, Kassmann CJ, Lo TP, Bruns CK, Powers ET, Kelly JW, Getzoff ED, Tainer JA. ALS mutants of human superoxide dismutase form fibrous aggregates via framework destabilization. J Molec Biol 2003;332:601–615.

24. Lindberg MJ, Bystrom R, Boknas N, Andersen PM, Oliveberg M. Systematically perturbed folding patterns of amyotrophic lateral sclerosis (ALS)-associated SOD1 mutants. PNAS 2005;102:9754–9759.
25. Rodriguez JA, Shaw BF, Durazo A, Sohn SH, Doucette PA, Nersissian AM, Faull KF, Eggers DK, Tiwari A, Hayward LJ, Valentine JS. Destabilization of apoprotein is insufficient to explain Cu,Zn-superoxide dismutase-linked ALS pathogenesis. Proc Natl Acad Sci USA 2005;102:10516–10521.
26. Ferraroni M, Rypniewski W, Wilson KS, Viezzoli MS, Banci L, Bertini I, Mangani S. The crystal structure of the monomeric human SOD mutant F50E/G51E/E133Q at atomic resolution. The enzyme mechanism revisited. J Molec Biol 1999;288:413–426.
27. Parge HE, Hallewell RA, Tainer JA. Atomic structures of wild-type and thermostable mutant recombinant human Cu,Zn superoxide-dismutase. Proc Natl Acad Sci USA 1992; 89:6109–6113.
28. Mcree DE, Redford SM, Getzoff ED, Lepock JR, Hallewell RA, Tainer JA. Changes in crystallographic structure and thermostability of a Cu,Zn superoxide-dismutase mutant resulting from the removal of a buried cysteine. J Biol Chem 1990;265:14234–14241.
29. Hart PJ, Liu HB, Pellegrini M, Nersissian AM, Gralla EB, Valentine JS, Eisenberg D. Subunit asymmetry in the three-dimensional structure of a human CuZnSOD mutant found in familial amyotrophic lateral sclerosis. Protein Sci 1998;7: 545–555.
30. Vorobjev YN, Hermans J. Free energies of protein decoys provide insight into determinants of protein stability. Protein Sci 2001;10:2498–2506.
31. Vorobjev YN, Hermans J. ES/IS: Estimation of conformational free energy by combining dynamics simulations with explicit solvent with an implicit solvent continuum model. Biophys Chem 1999;78:195–205.
32. Vorobjev YN, Almagro JC, Hermans J. Discrimination between native and intentionally misfolded conformations of proteins: ES/IS, a new method for calculating conformational free energy that uses both dynamics simulations with an explicit solvent and an implicit solvent continuum model. Proteins Struct Funct Genet 1998;32:399–413.
33. Vorobjev YN, Hermans J. Free energies of protein decoys provide insight into determinants of protein stability (vol. 10, p 2498, 2001). Protein Sci 2002;11:994.
34. Mann G, et al. The Sigma MD program and a generic interface applicable to multi-functional programs with complex, hierarchical command structure. In Schlick T, Gan HH, editors. New York: Springer-Verlag; 2002. pp 129–145. Computational methods for macromolecules: challenges and applications – Proceedings of the 3rd International Workshop on Algorithms for Macromolecular Modelling. 10-12-2000. Ref Type: Conference Proceeding.
35. Urbanc B, Cruz L, Ding F, Sammond D, Khare S, Buldyrev S, Stanley HE, Dokholyan NV. Molecular dynamics simulation of Amyloid beta dimer formation. Biophys J (2004).
36. Lindberg MJ, Bystrom R, Boknas N, Andersen PM, Oliveberg M. Systematically perturbed folding patterns of amyotrophic lateral sclerosis (ALS)-associated SOD1 mutants. Proc Natl Acad Sci USA 2005;102:9754–9759.
37. Rodriguez JA, Shaw BF, Durazo A, Sohn SH, Doucette PA, Nersissian AM, Faull KF, Eggers DK, Tiwari A, Hayward LJ, Valentine JS. Destabilization of apoprotein is insufficient to explain Cu,Zn-superoxide dismutase-linked ALS pathogenesis. Proc Natl Acad Sci USA 2005;102:10516–10521.
38. Fernandez-Escamilla AM, Rousseau F, Schymkowitz J, Serrano L. Prediction of sequence-dependent and mutational effects on the aggregation of peptides and proteins. Nat Biotechnol 2004;22:1302–1306.
39. Khare SD, Dokholyan NV. Common dynamical signatures of familial amyotrophic lateral sclerosis-associated structurally diverse Cu, Zn superoxide dismutase mutants. PNAS 2006; 103:3147–3152.
40. Khare SD, Wilcox KC, Gong P, Dokholyan NV. Sequence and structural determinants of Cu, Zn superoxide dismutase aggregation. Proteins Struct Funct Bioinformatics 2005;61: 617–632.
41. Foss TR, Wiseman RL, Kelly JW. The pathway by which the tetrameric protein transthyretin dissociates. Biochemistry 2005;44:15525–15533.
42. Hammarstrom P, Wiseman RL, Powers ET, Kelly JW. Prevention of transthyretin amyloid disease by changing protein misfolding energetics. Science 2003;299:713–716.
43. Merz GS, Benedikz E, Schwenk V, Johansen TE, Vogel LK, Rushbrook JI, Wisniewski HM. Human cystatin C forms an inactive dimer during intracellular trafficking in transfected CHO cells. J Cell Physiol 1997;173:423–432.
44. Janowski R, Kozak M, Abrahamson M, Grubb A, Jaskolski M. 3D domain-swapped human cystatin C with amyloidlike intermolecular beta-sheets. Proteins 2005;61:570–578.
45. Erlandsen H, Stevens RC. The structural basis of phenylketonuria. Molec Genet Metab 1999;68:103–125.
46. Waters PJ, Parniak MA, Akerman BR, Jones AO, Scriver CR. Missense mutations in the phenylalanine hydroxylase gene (PAH) can cause accelerated proteolytic turnover of PAH enzyme: A mechanism underlying phenylketonuria. J Inherit Metab Dis 1999;22:208–212.
47. Waters PJ, Parniak MA, Akerman BR, Scriver CR. How do missense mutations cause disease phenotypes? A paradigm for mechanism – and for modulation. Am J Hum Genet 1999;65: A497.
48. Olzmann JA, Brown K, Wilkinson KD, Rees HD, Huai Q, Ke HM, Levey AI, Li L, Chin LS. Familial Parkinson's disease-associated L166P mutation disrupts DJ-1 protein folding and function. J Biol Chem 2004;279:8506–8515.
49. Feil IK, Malfois M, Hendle J, van der Zandt H, Svergun DI. A novel quaternary structure of the dimeric alpha-crystallin domain with chaperone-like activity. J Biol Chem 2001;276: 12024–12029.
50. Aquilina JA, Benesch JLP, Ding LL, Yaron O, Horwitz J, Robinson CV. Phosphorylation of alpha B-crystallin alters chaperone function through loss of dimeric substructure. J Biol Chem 2004;279:28675–28680.